

Electronic Supplementary Information for:

Electronic engineering of a tetrathiafulvalene charge-transfer salt *via* reduced symmetry induced by combined substituents

Yasuhiro Kiyota,^{a,b} Ie-Rang Jeon,^{*b} Olivier Jeannin,^b Maxime Beau,^b Tadashi Kawamoto,^a Pere Alemany,^c Enric Canadell,^{*d} Takehiko Mori,^a Marc Fourmigué^{*b}

^a*Department of Materials Science and Engineering, Tokyo Institute of Technology, O-okayama 2-12-1, Meguro-ku, Tokyo 152-8552, Japan.*

^b*Univ. Rennes, CNRS, ISCR (Institut des Sciences Chimiques de Rennes) - UMR 6226, F35000 Rennes, France.*

^c*Departament de Ciència de Materials i Química Física and Institut de Química Teòrica i Computacional (IQTCUB), Universitat de Barcelona, Martí i Franquès 1, Barcelona 08028, Spain*

^d*Institut de Ciència de Materials de Barcelona (CSIC), Campus de la UAB, E-08193 Bellaterra, Spain*

e-mail: ie-rang.jeon@univ-rennes1.fr; canadell@icmab.es; marc.fourmigue@univ-rennes1.fr

Phys. Chem. Chem. Phys.

Table of Contents

| | |
|--|------------|
| Figure S1: Cyclic voltammogram of (Z,E)-1 | S2 |
| Table S1: Distances of the short contacts | S3 |
| Figure S2: NMR spectra of (Z,E)-1 and re-crystallized 1 by co-sublimation and sublimation | S4 |
| Figure S3: Powder diffraction pattern of [(E)-1](TCNQ) | S5 |
| Figure S4: Projection views of [(E)-1](TCNQ) | S6 |
| Figure S5: Energy levels of TTF derivatives and TCNQ | S7 |
| Table S2: Estimated charge-transfer degrees | S8 |
| Figure S6: Molecular structure of TCNQ | S8 |
| Figure S7: Temperature dependence of the resistivity and its derivative | S9 |
| Figure S8: Angle dependence of ESR signals | S10 |
| Figure S9: An illustration of a molecular arrangement with an inverse domain | S10 |
| Figure S10: Variation of the charge transfer with the effective Hubbard correction term U | S11 |
| Figure S11: Calculated band structure for TTF-TCNQ | S11 |
| Figure S12: Variation of the band widths (W) with the effective Hubbard correction term U | S12 |
| References | S12 |

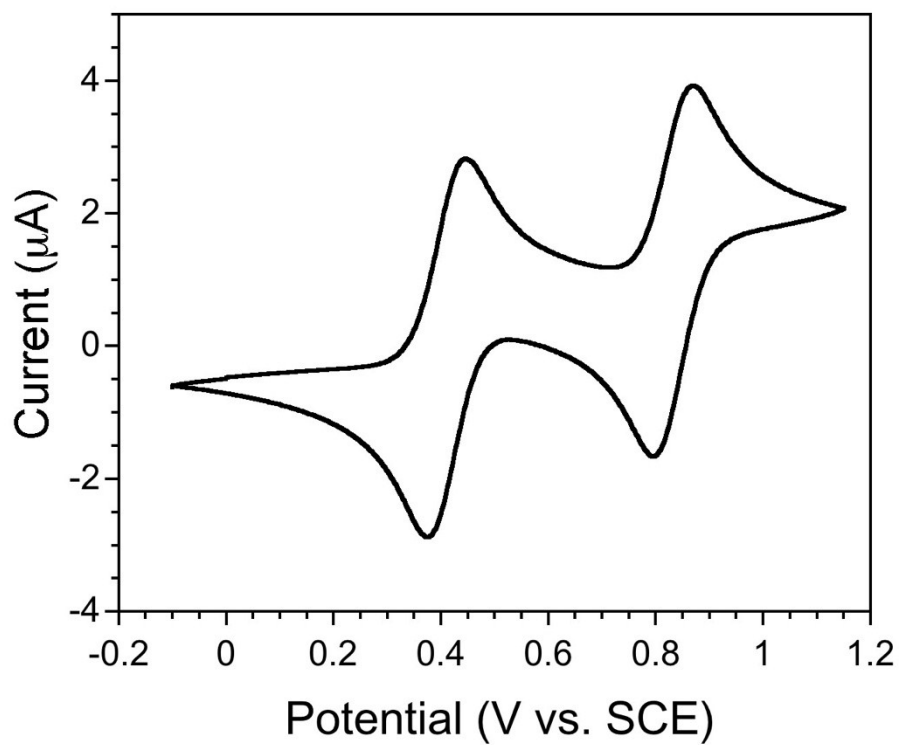


Figure S1 | Cyclic voltammogram obtained for a dichloromethane solution of (Z,E)-1 using a platinum electrode, 100 mV/s scan rate, and 0.1 M (Bu₄N)PF₆ supporting electrode: $E^{1/2} = +0.41$ V and $E^{2/2} = 0.83$ V.

Table S1 | Distances of the short contacts, C···C between acceptors and S···S between donors, along the chain direction in [(E)-1](TCNQ) and (TTF)(TCNQ).

| | [(E)-1](TCNQ) at 150 K | (TTF)(TCNQ) at room temp. |
|--|------------------------|---------------------------|
| C···C (Å) | 3.292 (×2) | 3.254 (×2) |
| | 3.307 (×2) | 3.260 (×2) |
| | 3.309 (×2) | 3.273 (×2) |
| | 3.341 (×2) | 3.278 (×2) |
| | 3.323 | 3.280 |
| S···S (Å) | 3.824 (×2) | 3.809 (×2) |
| | 3.842 (×4) | 3.819 (×4) |
| S_{outer}···S_{TTF} (Å) | 3.782 (×2) | - |
| S_{outer}···S_{outer} (Å) | 3.842 (×2) | - |

Experimental for the preparation of NMR samples

The NMR of the re-crystallized (*Z,E*)-**1** from EtOAc after the synthesis is shown in the red curve in Figure S2, exhibiting the mixture of *Z*- and *E*-isomers. During the co-sublimation, the glass tube containing both reactants and the product was completely sealed to avoid any loss of complexes. After sublimation process was over, we noticed that all orange microcrystalline solids of (*Z,E*)-**1** are sublimed and then a portion of it is recrystallized and another portion is co-crystallized with TCNQ. This can be checked by eyes from the position of the sample and the crystal quality that becomes much better after the sublimation. All the remaining orange-colored sample was dissolved in CDCl₃ by adding the solvent directly into the tube in order to represent the bulk. The obtained NMR spectrum (green curve in Figure S2) shows only *E*-isomer. The sublimation of (*Z,E*)-**1** alone without TCNQ has been done in two different conditions: 1) with cold-finger and 2) within exactly same condition as co-sublimation but without TCNQ. From the NMR, both conditions still afford mixture of two isomers (blue curve in Figure S2).

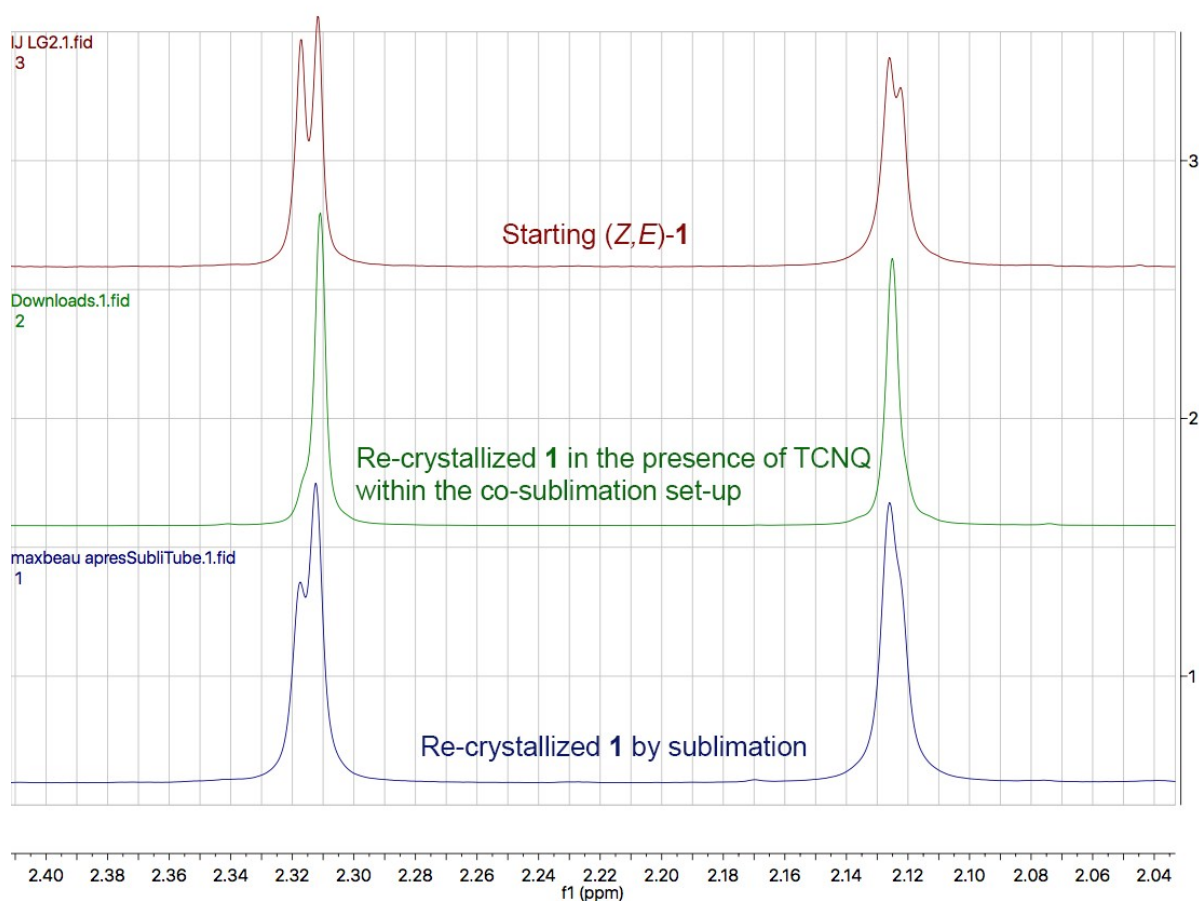


Figure S2 | NMR spectra of the starting (*Z,E*)-**1** (top), the re-crystallized **1** within the co-sublimation tube in the presence of TCNQ, and the re-crystallized **1** by sublimation without TCNQ.

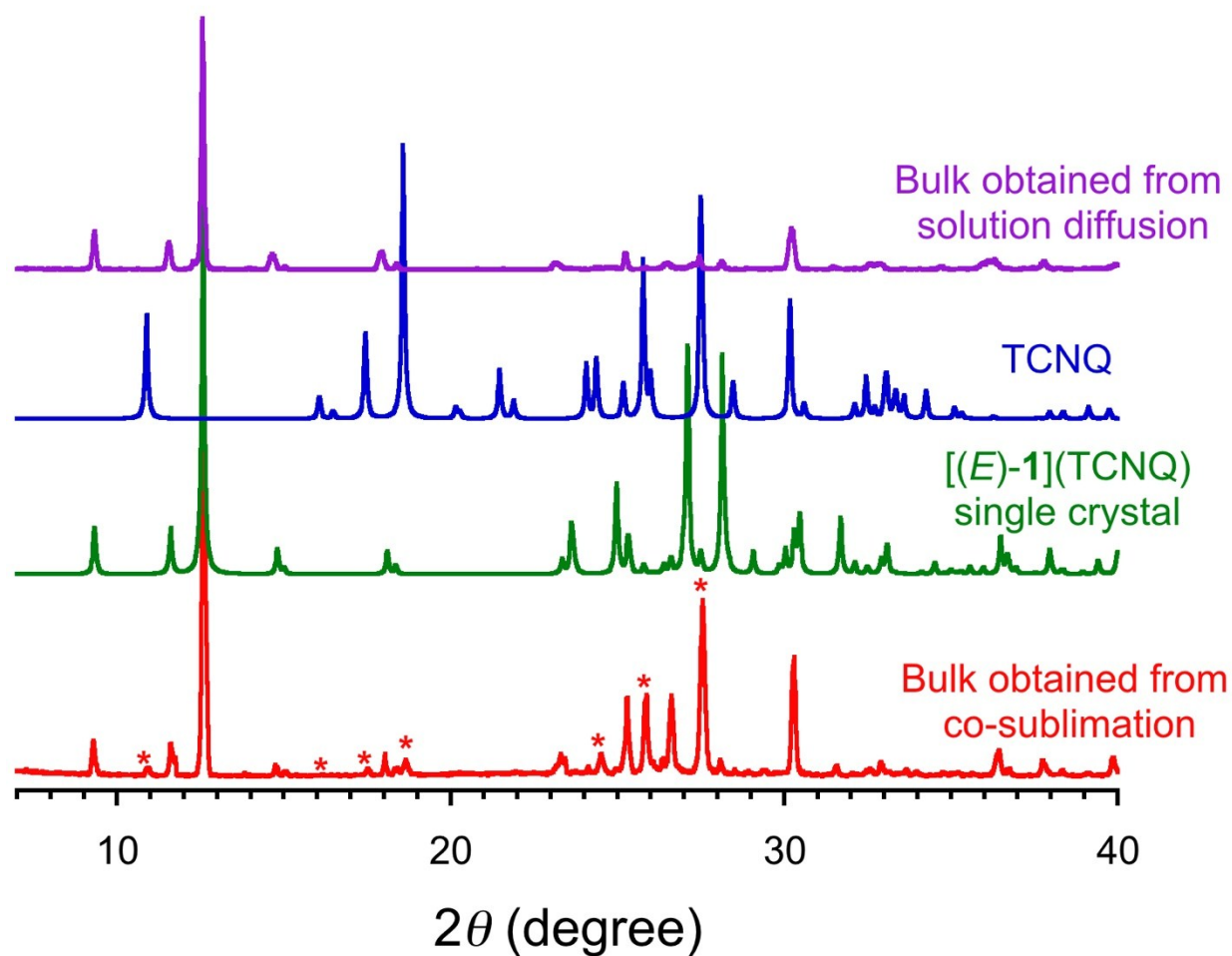


Figure S3 | Powder X-ray diffraction patterns of bulk material obtained from the co-sublimation (in red), that is compared with the simulated patterns of [(E)-1](TCNQ) single-crystal (in green), the TCNQ starting material (in blue), and the microcrystalline powder obtained by solution diffusion method (in purple). The red stars indicate the diffraction peaks corresponding to the TCNQ starting material.

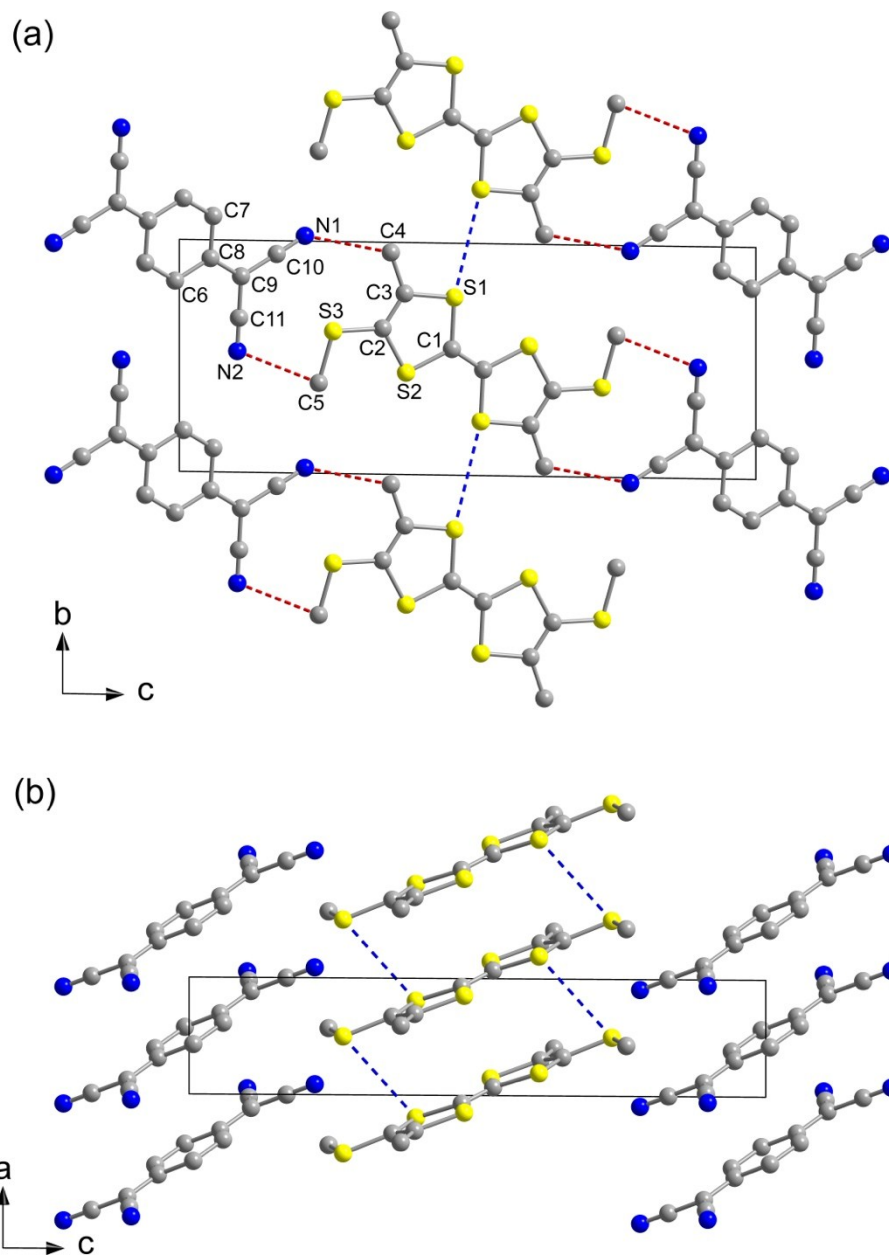


Figure S4 | Projection views of [(*E*)-1](TCNQ). Yellow, blue, and grey spheres represent S, N, and C atoms, respectively; H atoms are omitted for clarity. Short contacts described in the main text are shown in dashed lines.

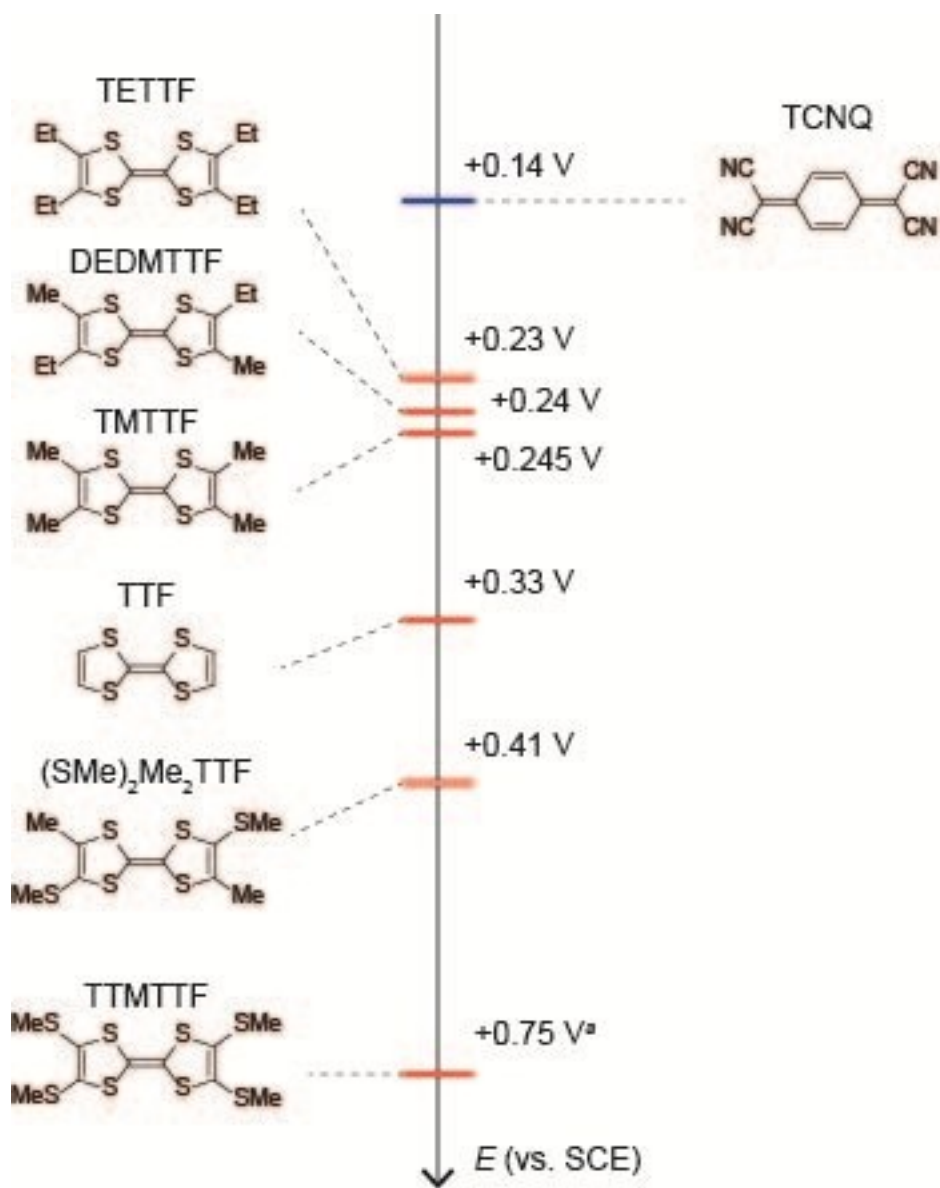


Figure S5 | Redox potentials of TTF, TETTF, DEDMTTF, TMTTF,^{S1} TTMTTF,^{S2} and TCNQ. ^aThe redox potential of TTMTTF is measured vs. Ag/Ag⁺ and collected by +0.2 V. ^{S2}

Charge-Transfer Degree

The charge-transfer degree ρ was estimated from the bond lengths b - d of TCNQ and the frequency of C \equiv N stretching mode of the IR spectra with using the following equations.^{S3,S4}

$$\rho_{\text{BL}} = -41.677 \times [c / (b+d)] + 19.818$$

$$\nu_{\text{C}\equiv\text{N}} = 2227 - 44\rho_{\text{IR}}$$

The results listed in Table S2 indicate that this CT salt has $\rho \sim 0.5$, hence this CT salt is recognized as nearly quarter filling.

Table S2 | A list of the bond lengths and the IR stretching frequency of TCNQ, and the charge-transfer degrees estimated from the bond lengths and the IR frequency.

| b (Å) | c (Å) | d (Å) | $\nu_{\text{C}\equiv\text{N}}$ (cm ⁻¹) | ρ_{BL} | ρ_{IR} |
|---------|---------|---------|--|--------------------|--------------------|
| 1.435 | 1.398 | 1.429 | 2201 | 0.52 | 0.59 |

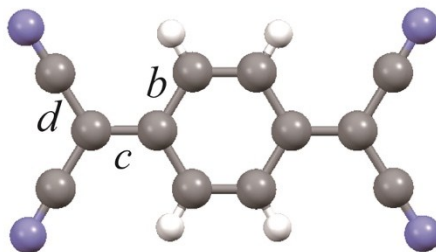


Figure S6 | Molecular structure of TCNQ; the bond lengths b - d are used for the estimation.

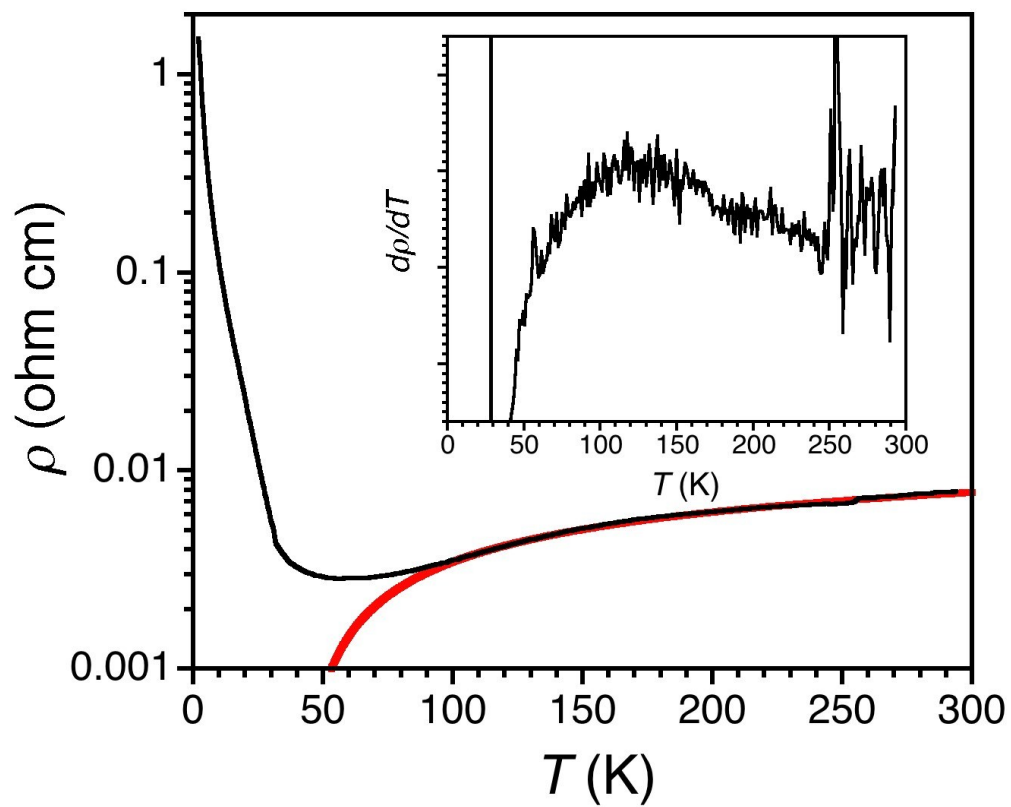


Figure S7 | Temperature dependence of the resistivity at 1 bar. Inset: the derivative of the resistivity.

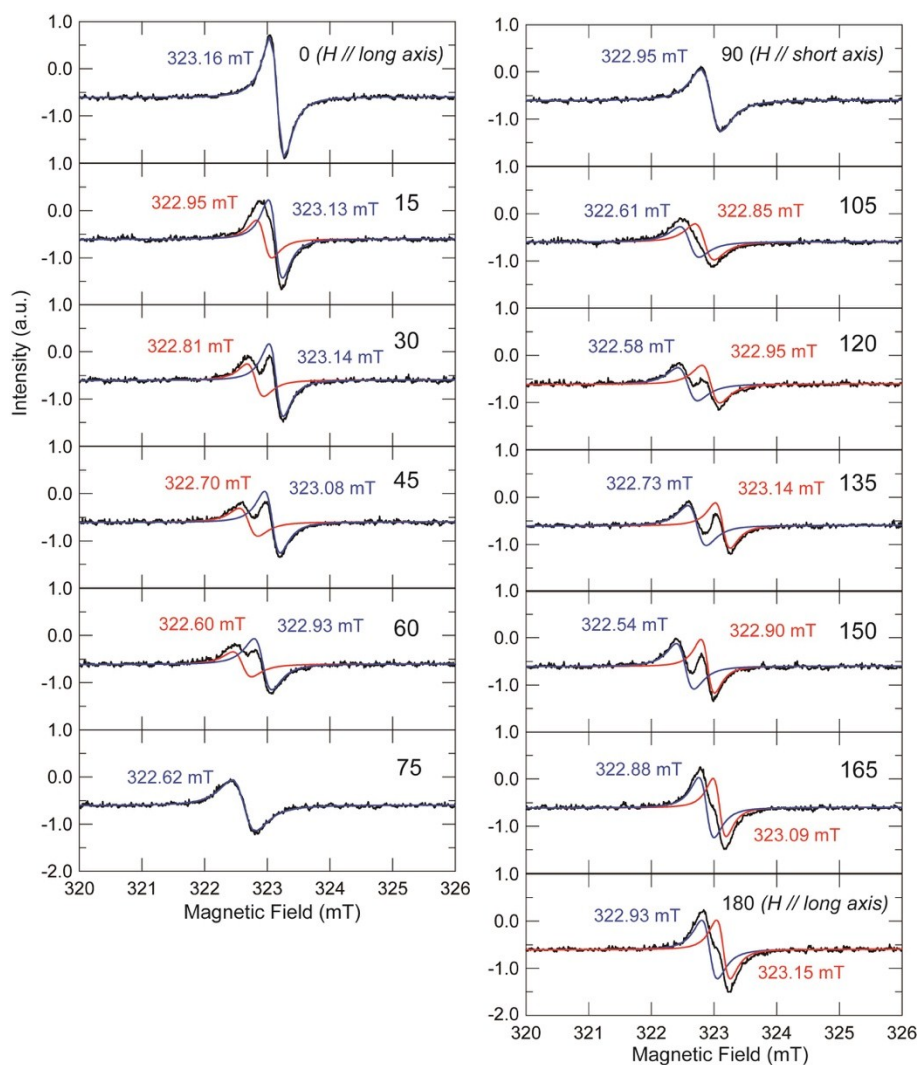


Figure S8 | Angle dependence of ESR signals.

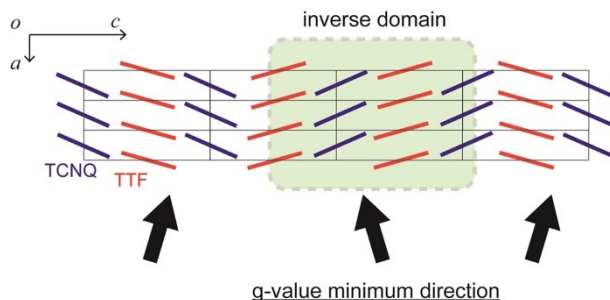


Figure S9 | An illustration of a molecular arrangement with an inverse domain viewed along the b -axis.

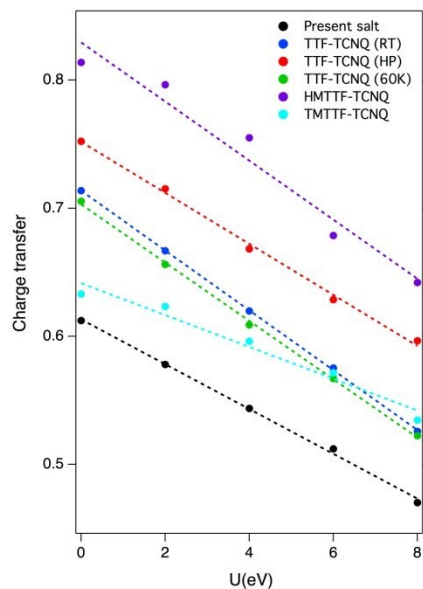


Figure S10 | Variation of the charge transfer with the effective Hubbard correction term U for different two-chain salts estimated from the k_F value disregarding the avoided crossing.

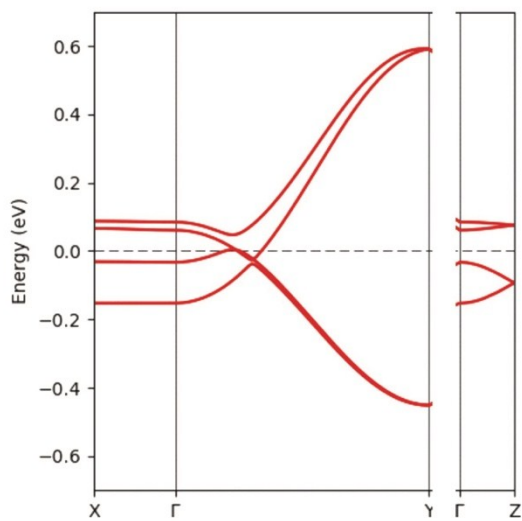


Figure S11 | Calculated band structure for TTF-TCNQ at room temperature and using $U=6$ eV. The Fermi level is the energy zero and $\Gamma=(0, 0, 0)$, $X=(1/2, 0, 0)$, $Y=(0, 1/2, 0)$, and $Z=(0, 0, 1/2)$ in units of the monoclinic reciprocal lattice vectors.

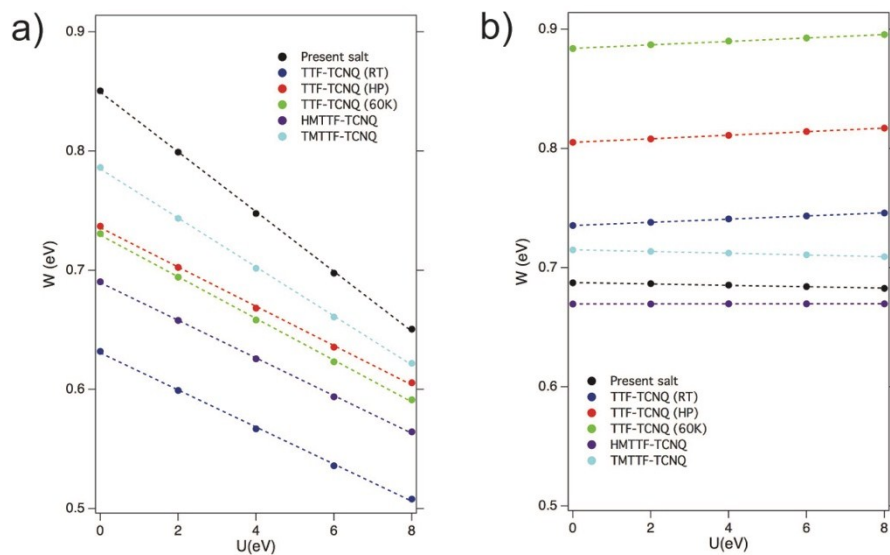


Figure S12 | Variation of the band widths (W) with the effective Hubbard correction term U for the donor (a) and acceptor (b) of different two-chain salts.

References

- S1 A. Mas, J. M. Fabre, E. Torreilles, L. Giral and G. Brun, *Tetrahedron Lett.*, 1977, **30**, 2579.
- S2 P. Wu, G. Saito, K. Imada, Z. Shi, T. Mori, T. Enoki and H. Inokuchi, *Chem. Lett.*, 1986, **15**, 441.
- S3 (a) T. J. Kistenmacher, T. J. Emge, A. N. Bloch and D. O. Cowan, *Acta Crystallogr., Sect. B: Struct. Sci.*, 1982, **38**, 1193; (b) K. Bechgaard, T. J. Kistenmacher, A. N. Bloch, *Acta Crystallogr., Sect. B: Struct. Sci.*, 1977, **33**, 417.
- S4 J. S. Chappell, A. N. Bloch, W. A. Bryden, M. Maxfield, T. O. Poehler and D. O. Cowan, *J. Am. Chem. Soc.*, 1981, **103**, 2442.